The Reaction Center Associated Tetraheme Cytochrome Subunit from *Chromatium vinosum* Revisited: A Reexamination of Its EPR Properties†

Wolfgang Nitschke,*,‡,§ Marc Jubault-Bregler,‡ and A. William Rutherford‡

Section de Bioénergétique, Département de Biologie Cellulaire et Moléculaire, CNRS URA 1290, CE Saclay, 91191 Gif sur Yvette Cedex, France, and Institut für Biologie II, Universität Freiburg, Schänzlestrasse 1, 79104 Freiburg, FRG

Received March 24, 1993; Revised Manuscript Received June 4, 1993

ABSTRACT: The heme components of chromatophore membranes from the purple bacterium *Chromatium vinosum* have been studied by EPR. Five different heme species could be distinguished on the basis of their *g* values, redox midpoint potentials, and orientations of heme planes with respect to the membrane plane: $g_z = 2.94$, $E_m = +10$ mV, 40°–50°; $g_z = 2.94$, $E_m = +10$ mV, 0°; $g_z = 3.1$, $E_m = +330$ mV, 90°; $g_z = 3.3$, $E_m = 360$ mV, 30°; $g_z = 3.4$, $E_m = 0$ mV, no detectable orientation. Four of these five hemes ($g_z = 3.3$, $g_z = 3.1$, and $2\times g_z = 2.94$) were ascribed to the tetraheme cytochrome subunit associated with the photosynthetic reaction center of this bacterium. Some of the results obtained have already been reported previously [Tiede, D. M., Leigh, J. S., & Dutton, P. L. (1978) *Biochim. Biophys. Acta 503*, 524–544] and have led to a model for the tetraheme cytochrome subunit in *Chromatium* which is significantly different from the three-dimensional structure of the reaction center associated subunit in the purple bacterium *Rhodopseudomonas viridis*. The additional data obtained in our work, however, require a reinterpretation of the previously published results. The model arrived at is in general agreement with the X-ray structure from *Rhodopseudomonas viridis*. A model rationalizing the detailed differences between the structure of the *Rhodopseudomonas viridis* cytochrome subunit and the data obtained on tetraheme subunits from other photosynthetic bacteria is presented.

In purple bacteria, photosynthetic electron transport from the cytochrome bc_1 complex to the photosynthetic reaction center (RC)[1] is usually mediated by the soluble carrier cytochrome c_2 (Wood, 1980). In most species of purple bacteria studied, however, cytochrome c_2 does not rereduce the photooxidized special pair (P^+) directly, but rather donates an electron to a reaction center associated multiheme cytochrome which in turn serves as the immediate electron donor to P^+ (Shill & Wood, 1984; Kihara & Chance, 1969; Matsuura & Shimada, 1990). The detailed mechanism of electron flow from cytochrome c_2 through this multiheme subunit into the reaction center is only poorly understood (Fukushima et al., 1988; Dracheva et al., 1988; Knaff et al., 1991; De Vault & Chance, 1966; Ortega & Mathis, 1992, 1993), and many aspects of this system remain enigmatic.

The crystal structure of the *Rhodopseudomonas viridis* reaction center allowed the structural organization of such a cytochrome subunit to be visualized for the first time (Deisenhofer et al., 1984; Deisenhofer & Michel, 1989). In *R. viridis*, it turned out to contain four heme groups arranged in a linear row protruding away from the reaction center into the aqueous phase.

Such a structure seemed optimally suited for electrochemical "downhill" electron transfer from the furthest heme into the RC. This idea, however, had to be discarded when it became clear that the four hemes were arranged in an alternating sequence of redox midpoint potentials (Shopes et al., 1987; Dracheva et al., 1988; Nitschke & Rutherford, 1989; Verméglio et al., 1989; Fritzsch et al., 1989; Alegria & Dutton, 1991; Gunner & Honig, 1991), i.e., in contradiction to linear electron flow through all four hemes toward P^+.

A subsequent study demonstrated that the overall organization of the *R. viridis* tetraheme subunit, i.e., four distinguishable hemes covering a wide range of redox potentials and oriented in a linear sequence, is also compatible with data obtained on the cytochrome subunit from another purple bacterium, i.e., from *Rhodocyclus gelatinosus* (Nitschke et al., 1992). In contrast to the reaction center core proteins L, M, and H, which appear to be highly conserved even with respect to structural details (Allen et al., 1986), the structure of the cytochrome subunit itself must be somewhat flexible, since the orientations of the four hemes found in *R. gelatinosus* as determined by EPR cannot be matched with those seen (both in the crystal structure and by EPR) for the *R. viridis* cytochrome subunit (Nitschke et al., 1992). In addition, the redox midpoint potentials of the four hemes in this bacterium differ significantly from those of the hemes in the *R. viridis* subunit (Dutton, 1971; Fukushima et al., 1988; Nitschke et al., 1992).

The existence of such general structural similarities in the tetraheme cytochrome of photosynthetic bacteria is also supported by earlier results obtained on *Chloroflexus aurantiacus* (Freeman & Blankenship, 1990; Van Vliet et al., 1991; Dracheva et al., 1991), a green gliding bacterium containing a purple bacterial-type reaction center and a tetraheme subunit which again is generally similar (Dracheva et al., 1991), however, with some variability with respect to both heme orientations and redox midpoint potentials of the individual hemes (van Vliet et al., 1991).

The data cited above therefore point toward the general applicability of the model derived from the *R. viridis* crystal

† A.W.R. is supported by the CNRS (URA 1290); W.N. is supported by the DFG.

* To whom correspondence should be addressed at the Institut für Biologie II, Universität Freiburg.

‡ CNRS URA 1290.

§ Universität Freiburg.

[1] Abbreviations: RC, reaction center; $E_{m,7}$, redox midpoint potential at pH 7.0; EPR, electron paramagnetic resonance; MOPS, 3-(*N*-morpholino)propanesulfonic acid.

0006-2960/93/0432-8871$04.00/0

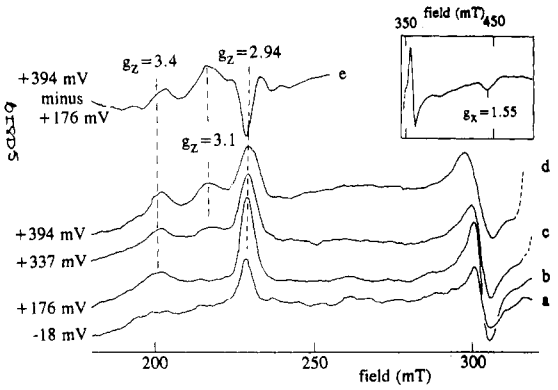

FIGURE 1: EPR spectra obtained on chromatophore membranes from *C. vinosum* poised at the following ambient redox potentials: −18 mV (a), +176 mV (b), +337 mV (c), and +394 mV (d). Spectrum e is a difference spectrum (expanded 2-fold with respect to spectra a–d) obtained by subtracting the spectrum recorded at +176 mV from that recorded at +394 mV. The inset shows the high-field spectral region of a sample poised at +176 mV. Instrument settings: temperature, 15 K; microwave power, 6.7 mW; microwave frequency, 9.45 GHz; modulation amplitude, 2.2 mT.

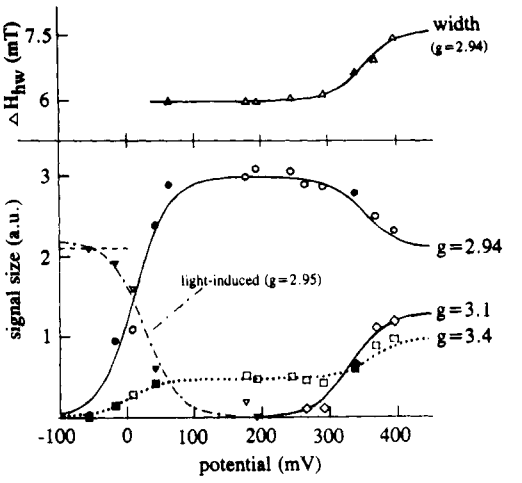

FIGURE 2: Redox titration at pH 7.0 of chromatophore membranes from *C. vinosum*. The signal intensities are plotted vs ambient redox potential for the peaks at g_z = 2.94 (○), g_z = 3.1 (◇), and g_z = 3.4 (□). The intensity of the signal at g = 2.95 which could be photoinduced at 4 K is denoted by (▽). The dependence on redox potential of the width at half-height measured for the peak at g = 2.94 is shown in the upper part of the figure (△). Data points obtained while titrating toward more positive and more negative potentials are denoted by open and filled symbols, respectively. The drawn curves are n = 1 Nernst functions fitted to the data points. The dashed level in the left part of the figure denotes the amplitude corresponding to one photoinduced g_z = 2.95 heme after correction for the narrower line width.

structure, but with fine-tuning of orientational and electrochemical parameters in different organisms.

However, on the basis largely of an EPR study, a strikingly different structural model was proposed for the tetraheme cytochrome from the purple bacterium *Chromatium vinosum* (Tiede et al., 1978). In this model, two pairs of identical hemes were thought to form two independent parallel pathways of electron transfer into the RC. Furthermore, in this model the two low-potential hemes (i.e., the so-called cyt c_{553} hemes) were proposed to be positioned closer to the RC than the high-potential pair (i.e., the cyt c_{555} hemes), whereas in *R. viridis*, the highest potential heme is apparently the closest one to the primary donor P.

In order to find out whether *Chromatium vinosum* actually differs from the *R. viridis* model, we undertook a reexamination of the tetraheme cytochrome subunit from *C. vinosum* taking advantage of the present knowledge gathered on the other tetraheme subunits studied so far.

EXPERIMENTAL PROCEDURES

Frozen harvested cells of *C. vinosum* (which were a gift from Dr. P. Heathcote) were resuspended in 50 mM MOPS (pH 7.0) and were subsequently disrupted by three passages through a French pressure cell.

Redox poising and redox titrations of chromatophore membranes (in 50 mM MOPS, pH 7.0, at an optical density of 60 at 800 nm) were performed in near-darkness under an appropriate safelight essentially as described by Dutton (1971). The following redox mediators were used: 1,4-benzoquinone, *N,N,N',N'*-tetramethyl-*p*-phenylenediamine, diaminodiurol, variamine blue, toluylene blue, 1,4-naphthoquinone, 5-hydroxy-1,4-naphthoquinone, duroquinone, indigotetrasulfonate, 1,4-dihydroxynaphthoquinone, 2,5-dihydroxy-*p*-benzoquinone, indigo carmine, 2-hydroxy-1,4-naphthoquinone, and safranine T at 100 μM; ferricyanide at 10 μM; phenazine methosulfate and phenazine ethosulfate at 50 μM. Reductive titrations were carried out using sodium dithionite, and oxidative titrations were done using porphyrexide (4-amino-2,5-dihydro-2-imino-5,5-dimethyl-1*H*-imidazol-1-yloxy).

Oriented membrane multilayers were obtained by using the technique of Blasie et al. (1978): membranes suspended in H_2O were painted on mylar sheets and were dried in 90% humidity atmosphere for approximately 24 h in darkness at 4 °C. The redox state in these membranes was adjusted by applying solutions of porphyrexide, sodium ascorbate, or sodium dithionite (all redox chemicals in 50 mM MOPS, pH 7.0) to the dried membranes followed by drying under a stream of argon gas in darkness. EPR spectra were recorded at liquid helium temperatures with a Bruker ER 300 X-band spectrometer, fitted with an Oxford Instruments cryostat and temperature control system.

Illumination in the EPR cavity was carried out by using a 800-W tungsten projector providing 16 000 $\mu E m^{-2} s^{-1}$ of white light at the EPR cavity window after being filtered through 2 cm of water and two calflex filters to remove infrared radiation.

The molecular models of the *R. viridis* cytochrome subunit were produced on a personal computer using the pdViewer software developed by H. H. Robinson and A. R. Crofts (Copyright, University of Illinois). Coordinates were obtained from the Brookhaven Data Bank (Bernstein et al., 1977; Abola et al., 1987; entry 1PRC).

RESULTS

Redox Behavior. Figure 1a–d shows EPR spectra recorded on chromatophore membranes from *C. vinosum* at ambient redox potentials ranging from −18 to +394 mV in the spectral range where g_z peaks of low-spin hemes are observed. The corresponding redox titrations for the g_z signals observed in the respective part of the spectrum are shown in Figure 2. The peaks at g = 2.94 and at g = 3.4 titrated at ambient potentials between −60 and +70 mV. The respective data points could be fitted by single n = 1 Nernst curves assuming E_m values of +10 mV for the g = 2.94 signal and of 0 mV for the g = 3.4 peak.

For the component giving rise to the g_z peak at 2.94, both of the other g factors could be observed at g_y = 2.2 and g_x = 1.55 (see inset in Figure 1 for the high-field part of the spectrum; the features between 350 and 400 mT are the g_y and g_x signals of the 2Fe2S center from the cytochrome bc_1 complex).

Although both the $g = 2.94$ heme and the $g = 3.4$ heme are possible candidates for one (or both) of the low-potential hemes, it is shown below that the $g = 3.4$ signal has isotropic orientation behavior, suggesting that the corresponding heme might be located in an only weakly membrane-attached component.

At ambient potentials above +250 mV, spectral changes at three different field positions could be seen. Most obvious was the appearance of a g_z peak at $g = 3.1$ (Figure 1c,d), with an E_m of +330 mV (Figure 2). Again, a single $n = 1$ Nernst curve fits the data satisfactorily. In addition, the peak at $g = 3.4$ increased about 2-fold and shifted toward slightly lower g values (Figure 1c,d; Figure 2). To obtain a pure spectrum of the species giving rise to the additional EPR absorption around $g = 3.3$ in the high redox potential range, the spectrum taken at E_h = +176 mV (i.e., at a potential where the high-potential hemes were reduced whereas the low-potential hemes were oxidized) was subtracted from the spectra obtained during the titration of the high-potential hemes (Figure 1, trace e). A comparison of such a difference spectrum and the absolute spectrum at 176 mV (Figure 1, trace b vs trace e) shows that the species titrating at about +360 mV (see Figure 2) was not identical to the low-potential, nonoriented heme with a g_z peak at 3.4 observable already at lower potentials.

It is of note that the signal amplitudes of g_z peaks are smaller at higher g factors in the observed range of magnetic fields. Using the semiempirical formula derived by de Vries and Albracht (1979), a stoichiometry of 0.66 ($g_z = 3.4$):0.75 ($g_z = 3.3$):1 ($g_z = 3.1$):1.8 ($g_z = 2.94$) was calculated. Thus, it seems likely that the $g_z = 2.94$ peaks results from the pair of low-potential hemes whereas the peaks at 3.3 and 3.1 correspond to the individual components of the high-potential pair of hemes.

In addition to the pure g_z peaks of the high-potential hemes, the spectrum in Figure 1e contains a derivative-shaped feature at the position of the low-potential hemes at $g = 2.94$. This derivative-shaped signal was due to a shift toward slightly lower g factors and a concomitant broadening of the $g = 2.94$ peak at potentials where the high-potential hemes are in the oxidized, paramagnetic state. The broadening and the decrease in amplitude of the $g = 2.94$ signal titrated at the same potential (+350 mV, Figure 2, compare titration curves at $E_h > 250$ mV) as did the high-potential hemes, strongly suggesting that these phenomena are related. The most straightforward explanation for this effect is provided by assuming an interaction between the low-potential hemes and the high-potential hemes.

Many of the data described above have already been reported by Tiede et al. (1978). However, our spin quantitations together with the orientational data shown below led us to arrive at different conclusions in some cases. A detailed comparison of our results with those presented by Tiede et al. is given under Discussion.

Orientational Properties. (A) The Low-Potential Pair of Hemes. The orientation dependence of the signal at $g = 2.94$ in the presence of ascorbate, i.e., when the high-potential hemes are in the reduced, diamagnetic state, is shown in Figure 3a (continuous line). The polar plot representation in this redox state might be taken to indicate that both low-potential hemes have their g_z directions oriented perpendicular to the membrane, i.e., that the hemes are parallel to the membrane plane (since the g_z direction in low-spin ferric hemes is close to perpendicular to the heme plane, an angle of α between g_z and the membrane translates into an angle of $90° - \alpha$ between the heme plane and the plane of the membrane). Therefore, two identical parallel hemes were assumed by Tiede et al. (1978).

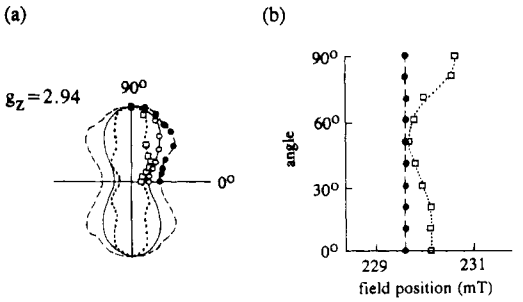

FIGURE 3: Dependence of signal amplitude (a) and signal position (b) of the $g_z = 2.94$ peak of the low-potential hemes on the angle of the magnetic field with respect to the plane of the membrane as measured in partially ordered membrane multilayers. (a) Signal amplitudes measured in the ascorbate-reduced state are denoted by open circles (continuous line). Open squares (dotted line) represent measurements performed on a sample where only 40% of the low-potential hemes are still in the oxidized state (the detailed sample treatment is described in the text). Filled circles (broken line) mark data points obtained on a fully reduced sample after illumination at 4 K. (b) The angular dependence of the position of the $g_z = 2.94$ peak is plotted for a sample in the ascorbate-reduced (filled circles, broken line) and in the porphyrexide-oxidized (open squares, dotted line) redox state.

The data discussed below, however, provide evidence for two distinguishable hemes with differing orientations.

The lobes of the polar plot appear relatively wide. This could indicate two differently oriented components, but equally it could be due to simply a poor orientation of the dried membranes, i.e., to a high mosaic spread (Blum et al., 1978). After measurement in the ascorbate-reduced state, the membrane sheets were dipped in 100 μM dithionite solution at pH 7 followed by rapid freezing in liquid N_2. The frozen sheets were then transferred to a freezer and incubated at –20 °C. Their reduction state was monitored by EPR once per day. Care was taken to assure that the sample was never warmed to above –20 °C. The applied dithionite solution very slowly reduced the low-potential components which give rise to the $g = 2.94$ peak. After 1 week of this treatment, the $g = 2.94$ peak was virtually absent. During the course of this slow reduction process, orientation studies were performed at various degrees of reduction of the low-potential hemes. The dotted line in Figure 3a shows the respective orientation dependence at the state when about 40% of the low-potential hemes were still oxidized. In this curve, the region around 90° had narrowed significantly, and a side maximum at around 40° became visible. The contribution of this side maximum seemed to become more prominent at higher degrees of reduction, yet the poor quality of the polar plots at these redox states (due to the very small signal amplitudes) made reliable evaluations impossible.

However, even at the highest degrees of reduction examined, the 90° component was still the dominant one. These results can be rationalized by assuming two differently oriented low-potential hemes which titrate with almost, but not exactly, the same redox midpoint potential. The signal of the 90° g_z component is dominant for the following geometrical reason: Since the samples are only two-dimensionally ordered, all orientations are degenerate with respect to C_∞ rotations around the membrane normal as the symmetry axis; i.e., the population of hemes at an angle α will be equally distributed around the membrane normal, and their g_z directions will form a cone of width α around this normal. However, the EPR experiment detects only that fraction of molecules on this cone which point their g_z vectors approximately (i.e., within the width of the mosaic spread) in the direction of the magnetic field. Hemes which are oriented parallel to the membrane (i.e., which point

their g_z direction perpendicular to the membrane) represent a unique situation since for this case the cone collapses to a line and virtually all molecules contribute to the observed spectrum. This yields a singularly high amplitude for the g_z peak of "parallel hemes" when the magnetic field is normal to the membrane plane.

The decreasing proportion of the 0° heme while reducing the low-potential pair of hemes seemed to indicate that its E_m was slightly more positive than that of the second low-potential heme. However, this conclusion is not firm since differential accessibilities of the respective heme moieties for dithionite would result in a similar effect.

The second low-potential heme (which is inclined toward the membrane) became rather clearly visible in low-temperature photooxidation experiments (Figure 3a, dashed line; for details, see section on 4 K photooxidation).

An accurate determination of the angle of inclination for this second low-potential heme was hampered by the overlap from the 0° component. An inspection of the polar plots in Figure 3 (dashed–dotted lines), however, indicated an angle of 40°–50° between the g_z direction and the membrane plane.

For the g_y and the g_x signals, the polar plots showed broad lobes with maxima approximately in the plane of the membrane (not shown). The signal-to-noise ratio for these lines, however, was insufficient to repeat the evaluation performed for the g = 2.94 peak.

If the two hemes were only approximately but not exactly at the same field position, their different orientations could in principle result in orientation-dependent field positions. Within experimental accuracy, such effects were absent for the case of the ascorbate-reduced samples, i.e., when the high-potential hemes were in the reduced, diamagnetic state (Figure 3b, dashed curve). However, in fully oxidized (i.e., porphyrexide-treated) membrane samples, where all hemes are paramagnetic, pronounced changes could be observed. As already described above (section on redox behavior), under comparably oxidizing conditions in nonordered samples, the g_z = 2.94 peak of the low-potential hemes shifted toward higher magnetic fields and broadened significantly (see Figures 1 and 2), most probably due to interaction with one or both of the high-potential hemes (for considerations with regard to the nature of this interaction, see Discussion). In the oriented samples, such broadening effects were less obvious. Instead, the g_z peak moved by 1.1 mT on rotation of the sample. A plot of this effect is shown in Figure 3b (dotted line). The signal position came close to that seen in the ascorbate-reduced, noninteracting case only at around 50°. This suggested that the 40°–50° heme was not or was only weakly interacting with other hemes. By contrast, the line shift as compared to the ascorbate-reduced samples was maximal when measured perpendicular to the membrane, indicating that it is the 0° heme which was strongly affected by interaction and which caused the line broadening seen in the nonoriented samples. Thus, the apparent broadening of the peak at g = 2.94 can actually be explained by less overlapping peak positions of two different hemes. In the oriented sample, the apparent line broadening was less pronounced because (due to the geometric effect, see above) the 0° heme dominates the spectrum.

(B) The High-Potential Pair of Hemes. As described above, two g_z peaks at g = 3.3 and g = 3.1 could be ascribed to the high-potential pair of hemes. The dependence of signal amplitude vs orientation for the g = 3.1 signal is shown in Figure 4a. The g_z peak was maximal when the magnetic field was roughly parallel to the membrane plane; i.e., it must arise from a heme which itself is oriented perpendicular to the parent membrane.

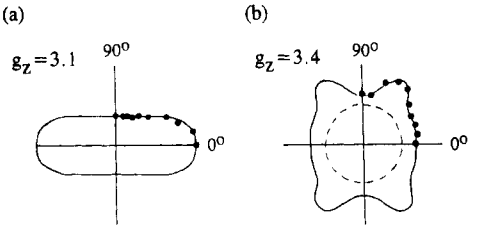

FIGURE 4: Polar plots of the signal amplitudes of the two high-potential hemes at g_z = 3.1 (a) and g_z = 3.4 (b) as measured in oriented membrane multilayers in the porphyrexide-oxidized state. In (b), the contribution of the 0-mV heme as seen in the ascorbate-treated membranes is indicated by the dashed line.

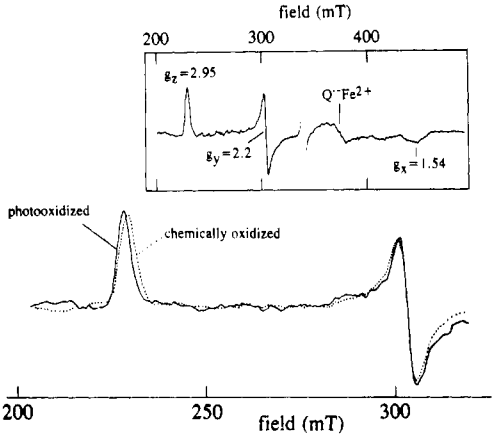

FIGURE 5: EPR spectrum photoinduced at 4 K in a sample which was in a highly reduced redox state (E_h = –60 mV) prior to illumination). For comparison, the spectrum of a sample at an ambient potential where the low-potential hemes are in the oxidized state (E_h = +176 mV) is indicated by a dotted line. The inset shows the complete spectrum of the photoinduced heme together with spectral features arising from the photoreduced $Q_A^{\cdot-}$-Fe^{2+} electron acceptor. Instrument settings are as described in Figure 1. These measuring conditions are not optimized for the observation of the semiquinone–iron signal, hence its relatively low amplitude.

As with the nonordered sample, the peak at g = 3.4 was seen in oriented multilayers already in the ascorbate-reduced state. The orientation dependence of this signal, however, was isotropic and therefore probably does not result from a firmly membrane-associated cytochrome. By contrast, when the membranes were treated with porphyrexide, the signal increased in size and became orientation-dependent with a maximum around 60° (Figure 4b). Thus, the respective high-potential heme must lie at about 30°–40° with respect to the membrane plane.

4 K Photooxidation Properties. As already observed previously (De Vault & Chance, 1966; Kihara & Dutton, 1970; Dutton & Leigh, 1973; Tiede et al., 1978; Heathcote & Rutherford, 1987), a stable charge separation between Q_A^- and one of the low-potential hemes can be light-induced at cryogenic temperatures (down to 2 K) in samples where all four hemes are reduced prior to illumination.

Figure 5 shows light minus dark difference spectra of the photooxidized low-potential heme. The full spectrum (i.e., all three g factors) of the photooxidized heme together with the signal resulting from the photoreduced secondary acceptor Q_A (the so-called semiquinone–iron signal) could be observed (Figure 5, inset). The g_z peak of the photooxidized heme (solid line) was not identical to the signal seen during equilibrium redox titrations (dotted line). The photoinduced peak is narrower by a factor of 0.75 and is shifted toward

lower magnetic fields. This altered peak position can be rationalized in two different ways: (a) During the equilibrium redox titration, populations having either one or the other or both of the two low-potential hemes oxidized in one molecule coexist due to the close E_m of the two low-potential species. The populations containing two oxidized hemes in the same molecule could give rise to interaction-induced spectral changes which would be absent in the photooxidation experiment since only one electron can be extracted from the four-heme system. (b) The microconformation around the respective heme moiety might be different when the low-potential hemes are oxidized compared to when they are reduced. Thus, illumination at low temperature would photooxidize a heme molecule which is in a microenvironment of the fully reduced state. If this conformation cannot relax at 15 K into the "one-heme-oxidized" conformation, then the spectrum of the heme might well be different from the spectrum obtained during the titration.

We favor interpretation b. Model a would predict that the signal observed in equilibrium titrations at very low degrees of oxidation of the low-potential hemes should approach the photooxidized signal, since in this case the probability of having molecules with two hemes oxidized should become negligible. No such spectral changes could be observed during redox titrations.

The redox potential dependence of the photoinduced increase in signal amplitude of the $g = 2.94$ peak is shown in Figure 2 (dot–dashed line). The maximal photoinduced amplitude is considerably higher than 50% of the amplitude seen in equilibrium redox titrations of the two low-potential hemes. This can be rationalized by the narrower line width. The measured amplitude corresponds roughly to the value predicted by taking the correction factor of 1.4 (correcting for the narrower line width) into account (dashed level in Figure 2).

Fitting an $n = 1$ Nernst curve to the data points yielded an E_m value of $+30 \pm 20$ mV for the photoinduced $g = 2.95$ signal.

The orientation dependence of the g_z peak photoinduced at 4 K in samples where all hemes were chemically reduced prior to illumination is shown in Figure 3a, dashed line. The 40°–50° heme was the prominent photooxidized species. Since the 0° species yields a significantly higher amplitude than inclined hemes at the same spin concentration (see above), it was most probably photooxidized only to a rather small extent. However, it is clear that the positive charge injected into the tetraheme system as a result of the 4 K illumination does not end up at the same heme in all cytochrome molecules. In the majority of the centers, the 40°–50° heme is oxidized, and in a minor fraction of centers, the positive charge is trapped on the 0° species. Warming of the sample up to 100 K did not result in a redistribution of charge on these hemes. Therefore, this effect seemed to be different from the situation encountered in *R. viridis* (Nitschke & Rutherford, 1989), where photooxidation at 4 K in the fully reduced state resulted in complete oxidation of the +20-mV heme (second away from the RC) whereas warming to 60 K allowed further migration of the positive charge to the −80-mV heme (fourth heme from P). In the case of *C. vinosum*, the described effect instead seemed to arise from microheterogeneity within the heme system which may be related to the very close E_ms of the two low-potential hemes.

It is of note that no light-induced changes at low redox potentials were detected around $g = 3.4$. This further argues against any implication of this heme in the low-potential pair of hemes within the tetraheme subunit.

Table I: Spectral, Orientational, and Electrochemical Parameters of the Hemes Observed in Chromatophore Membranes from *C. vinosum*

			orientation with respect to membrane (deg)	
g value	stoichiometry	$E_{m,7}$ (mV)	g_z	heme
2.94	0.9	≈+10 (−10)[a]	50–40 ± 20	40–50 ± 20
2.94	0.9	≈+10 (+30)[a]	90 ± 10	0 ± 10
2.95	*b*	+30 ± 20		mainly 40–50
3.10	1.0	+330 ± 20	0 ± 10	90 ± 10
3.30	0.75	+360 ± 30	60 ± 10	30 ± 10
3.40	0.66	0 ± 30	*c*	*c*

[a] The individual E_m values for the low-potential hemes are deduced from the work of Case and Parson (1973) as described in the text. [b] Photoinduced. [c] No detectable orientation.

DISCUSSION

The orientational and electrochemical parameters determined in this study for the five major hemes of chromatophore membranes from *C. vinosum* are summarized in Table I. Four of these hemes very likely constitute the RC-associated tetraheme subunit of this bacterium. Each of these four hemes is characterized by a unique set of EPR spectra, redox midpoint potentials, and orientations with respect to the membrane. No pair of identical hemes could be found.

Although the fifth heme (peaking at $g = 3.4$) could, on the basis of its redox midpoint potential ($E_m = 0$ mV), represent one of the two low-potential hemes, this seems unlikely for the following reasons: (1) this heme seems to be nonoriented; (2) it does not participate in low-temperature photooxidation; and (3) the peak at $g = 2.94$ (which corresponds to the low-temperature photooxidizable heme) already seems to consist of two distinguishable low-potential hemes.

Comparison to Previous Studies. In 1978, Tiede et al. performed a similar study on the cytochrome subunit from the same organism and were led by their data to propose two pairs of identical hemes, i.e., the low-potential pair (which appeared to be parallel to the membrane) and the high-potential pair (seen as perpendicular to the membrane). The data obtained in this early study by EPR of an RC-associated cytochrome subunit must be corrected in a few details which, however, change the final model considerably:

(a) Similar to Tiede et al., we attribute the $g = 2.94$ peak to the pair of low-potential hemes (cytochrome c_{553}). Like Tiede et al., we were unable to distinguish the two low-potential hemes on the basis of an equilibrium redox titration. Even so, slight E_m differences can be inferred by the observation that in oriented membranes, the 0° heme is more easily reduced than the 40°–50° heme.

No matter how small the E_m difference might be, in our study the two low-potential hemes are distinguishable on the basis of their orientations with respect to the membrane (however, also see Interaction Properties section). That the 40°–50° heme had escaped detection in the previous study is probably due to large variations in the maximal signal amplitude as a function of heme orientation. As detailed above, the signal amplitudes of g directions which are oriented perpendicular to the membrane are uniquely high. Therefore, they render the observation of differently oriented signals peaking at the same magnetic field position rather difficult.

The two low-potential hemes can furthermore be distinguished by their dissimilar interaction with the high-potential hemes; only the 0° heme seems to interact detectably with one or both of the high-potential hemes, and no significant broadening of the individual hemes of the low-potential pair seems to occur. This finding is at variance with the conclusions

drawn by Tiede et al., who interpreted the line broadening solely on the basis of magnetic interaction. For a more detailed discussion of this point, see Interaction Properties.

(b) Tiede et al. attributed the $g_z = 3.1$ peak to both of the high-potential hemes, since no other component titrating in the respective range of ambient potentials was found. Since this peak is oriented parallel to the membrane, they concluded that both high-potential hemes are perpendicular to the membrane plane. In 1978, when Tiede et al. performed their study, no straightforward relationship relating field position and signal amplitude had been demonstrated. However, in 1979, de Vries and Albracht proposed a semiempirical description of this relationship. Applying this algorithm to the spectra under consideration shows that the $g = 3.1$ peak cannot account for the same amount of spins as does the $g = 2.94$ peak of the low-potential pair (see quantitations under Results). Instead, the $g = 3.1$ peak corresponds to roughly one heme, and the missing second high-potential heme gives rise to a signal at $g = 3.3$ which titrates around +360 mV. An increase in intensity of this peak is actually visible in Tiede et al.'s work (see Figures 1–3 of this reference), and it was probably only the low signal amplitude (which is due to the high g value) and the fact that a signal is present at roughly the same position already at low ambient potentials which made these authors disregard this signal as a possible candidate for the tetraheme cytochrome.

Therefore, in addition to the perpendicular high-potential heme already seen by Tiede et al., a second high-potential heme exists which lies at a rather low angle (30°) toward the membrane. In our study, the E_m of this heme and consequently its denomination as the highest potential heme have a rather high uncertainty due to the low signal intensity. However, a recent optical study on Langmuir–Blodgett films of reaction centers from *C. vinosum* (Alegria & Dutton, 1990) yielded an E_m of +372 mV for the highest potential heme which is reasonably close to our value.

Early optical and EPR studies on the cytochromes involved in photoinduced electron donation to the reaction center in a variety of purple bacteria (Parson, 1969; Dutton, 1971; Case & Parson, 1973; Prince et al., 1976; Tiede et al., 1978) only distinguished between the so-called high- and low-potential groups of hemes. Nevertheless, it was clear that more than one heme of each group was present per reaction center. The inability to distinguish nonequivalent subpopulations within each group led to the model of identical hemes competing for the same reaction center (Dutton & Prince, 1978). Multiple flash experiments, however, showed inequivalent midpoint potentials for the first and the second flash-induced heme oxidations. This effect was rationalized by a mathematical model assuming several identical hemes per reaction center (Case & Parson, 1971; Jackson & Dutton, 1973). In this model, the difference in redox midpoint potential between the first and the second flash-induced cytochrome oxidation is a function of the number of hemes per RC.

To our knowledge, the validity of this interpretation for the multiple flash experiments has not been questioned to date. However, the present knowledge strongly suggests that the determined redox potentials should be taken at face value, i.e., reflecting actual equilibrium midpoint potentials of inequivalent hemes. This is for the following reasons: (a) From the variations in E_m differences of first and second flash oxidations between species of purple bacteria, the model described above would yield different stoichiometries of hemes per RC depending on species. However, in all purple bacteria examined in sufficient detail which contain RC-bound cytochrome subunits, this subunit always seems to be a tetraheme cytochrome. (b) The titration curves for the multiple flash oxidations of hemes in *R. viridis* measured by Prince et al. (1976) perfectly match the values which have been determined for the individual hemes of the *R. viridis* tetraheme subunit during recent years.

It is therefore reasonable to reinterpret multiple flash data obtained on *C. vinosum* (Case & Parson, 1971, 1973) to reflect the true E_m values of the individual hemes. This yields the following potentials: +360, +320, +28, and −12 mV. The two higher E_m values are in good agreement with our results. The E_m difference of 40 mV for the low-potential pair of hemes would be too small to be observable in our titration curve. The E_m of +10 mV found for the $g_z = 2.94$ peak, however, matches well the average E_m of +8 mV reported by Case and Parson (1971). Therefore, we suggest that the lowest potential heme (which probably corresponds to the 40°–50° heme) and the second lowest heme (possibly corresponding to the parallel heme) have individual E_m values of about −10 and +30 mV, respectively.

Interaction Properties. To rationalize the extent of the observed broadening of the $g_z = 2.94$ peak by magnetic interaction, Tiede et al. had to assume a distance of as low as 8 Å between interacting spins (i.e., between the Fe atoms of the high- and low-potential hemes). This close distance cannot be reconciled with the *R. viridis* structure.

Our orientation results, however, suggest that the spectral changes were due to a spectral shift of only one of the two low-potential hemes (i.e., the 0° heme), rather than a general broadening of this g_z peak.

Such spectral shifts can arise from electrostatic interaction of paramagnets with neighboring charges [see Mims and Peisach (1976)], as already noted by Tiede et al. (1978). Depending on the choice of dielectric constant, the observed shifts (1.1 mT) would, if due to electrostatic interaction, predict distances between paramagnet and neighboring charge in the region of 10–20 Å. This is in good agreement with the average Fe–Fe distance in the *R. viridis* cytochrome subunit (about 14 Å).

The fact that it is the 0° heme only which displays measurable interaction effects makes it rather likely that this heme is one of the two middle hemes in the subunit. The sequences low-potential heme (40–50°) ↔ high-potential heme ↔ low-potential heme (0°) ↔ high-potential heme and low-potential heme (40–50°) ↔ low-potential heme (0°) ↔ high-potential heme ↔ high-potential heme are both in line with a stronger effect on the 0° component upon variations of the electrostatic potential induced by oxidation/reduction of the high-potential hemes.

As shown in the study by Mims and Peisach (1976), the magnitude of the electric field induced spectral shift can depend on the angle between the external magnetic field and the internal electric field. Although we consider it quite unlikely that this effect would coincide by chance with the angles determined for the two low-potential heme components, it cannot be fully excluded that the orientation-dependent field positions shown in Figure 3b are due to such anisotropic interaction rather than reflecting two different populations. This would remove one piece of information with regard to the more detailed arrangement of hemes. The general properties of the structural model outlined below, however, would not be affected.

Heterogeneity. The 4 K photooxidation data show that even in a sample which is in a homogeneous redox state (i.e., all four hemes reduced, Q_A fully oxidized), the charge-

separated state after illumination is not identical in all centers. Most of the centers undergo charge separation between the 40°–50° heme and Q_A whereas a smaller but still measurable fraction of charge separation results in oxidized 0° hemes. Therefore, the sample seems to be conformationally heterogeneous, with different populations of molecules reacting differently from each other. Such conformational heterogeneity has already been evoked to explain low-temperature photoreaction results in *R. viridis* (Gao et al., 1990; Ortega & Mathis, 1992, 1993) and *R. gelatinosus* (Nitschke et al., 1992).

Structure of the Tetraheme Subunits from Purple Bacteria. The data described above resolve a longstanding controversy between the model derived for the tetraheme subunit of *C. vinosum* (based on EPR data) and the three-dimensional structure of the reaction center from *R. viridis* (Deisenhofer et al., 1989). The presence of distinguishable hemes and the interaction distances are in agreement with the linear row of hemes pointing away from the RC into the periplasmic space as seen in the *R. viridis* crystal structure and cannot be accommodated in the previous model of two identical parallel electron-transfer pathways. Thus, the *R. viridis* structure is most probably generally valid also for the heme subunit from *C. vinosum*.

However, the analogy does not hold on the level of conformational details for the four hemes. In *R. viridis*, the heme closest to the RC turned out to be nearly perpendicular, the two subsequent hemes were inclined by about 45° toward the membrane plane, and the last, furthest heme was again close to perpendicular. The ordering of redox midpoint potentials was determined to be RC → first high-potential heme → first low-potential heme → second high-potential heme → second low-potential heme. In *C. vinosum*, only one perpendicular heme is present, and this heme apparently is the one with only the second highest potential. The highest potential heme lies at a rather low angle (30°) with respect to the membrane.

The two low-potential hemes also could be distinguished into a parallel heme and one which is at a relatively steep angle with respect to the membrane plane.

In the absence of a crystal structure for the *C. vinosum* subunit and due to the lack of detailed similarities between the data obtained here and those gained for the *R. viridis* subunit, considerations of possible heme arrangements are necessarily speculative. Nevertheless, it seems reasonable to assume that one of the two high-potential hemes serves as the immediate donor to the photooxidized special pair of bacteriochlorophylls, i.e., is closest to P. Furthermore, in all systems performing electron transfer between a cytochrome and a special pair examined so far (Deisenhofer et al., 1989; Tiede, 1987; Tiede & Chang, 1992), the immediate donor always seems to be nearly perpendicular to the membrane, thereby creating a geometry which results in edge-to-edge electron transfer between heme and chlorophyll. Assuming that this rule also holds for the case of the *C. vinosum* cytochrome subunit, we conclude that for efficient electron transfer to P, it might not be strictly necessary for the closest (donating) heme to be the one which has the highest redox potential as measured in equilibrium redox titrations. The same situation may exist in *R. gelatinosus*, where again the perpendicular high-potential heme is only the second in potential (Nitschke et al., 1992).

The most "parsimonious" way to correlate the orientational data obtained in this work for the *C. vinosum* hemes and those reported previously for the hemes in *R. gelatinosus* (Nitschke et al., 1992) to the structure of the *R. viridis* RC would be to assume an almost unaltered structure of the protein but a slightly different way of attachment of the cytochrome subunit to the RC. In *R. viridis*, the elongated tetraheme protein is asymmetrically attached to the RC, and its local C_2 axis of symmetry is at an angle of about 30° with respect to the membrane plane. The surface of attachment of the cytochrome subunit to the RC in *R. viridis* is largely made up from two sequence stretches (see Figure 6a) which both break the local C_2 symmetry of the tetraheme protein [a symmetry which is proposed to be due to the evolution of the tetraheme cytochrome subunits from a gene-duplicated diheme protein; see Weyer et al. (1987)]. In Figure 6a,b, these sequence stretches are encircled by dotted lines. On the right hand side of the cytochrome subunit (Figure 6a), an N-terminal part is present which first winds along the membrane plane (residues 1–25), then protrudes vertically away from the membrane toward the far end of the cytochrome subunit (residues 26–44), and winds around this far end before joining the C_2 symmetric part of the protein (residues 45–55). The C_2 symmetry is further broken by the stretch of amino acids between residues 202 and 226 forming a loop along the surface of the membrane (on the left in Figure 6a,b). Looking vertically down from the membrane plane onto the tetraheme subunit from *R. viridis* (Figure 6b) shows that these two structural elements are located on approximately opposite sides of the protein. It is therefore tempting to consider interspecies differences within these two patches which would entail variations in tilt angles of the subunit along a plane indicated by the dashed line in Figure 6b. Such varying tilt angles would leave the orientations of the nearest and the furthest heme from the RC roughly unaltered (i.e., not far from perpendicular to the membrane) and would essentially only affect the orientations of the two middle hemes. If this inclination was made slightly steeper (by 20°–30°) than observed in *R. viridis* (see Figure 6c), then the two middle hemes (about 45° in *R. viridis*) would become almost parallel to the membrane plane, and the pattern of heme orientations would correspond roughly to that obtained experimentally for the hemes in *C. vinosum* and *R. gelatinosus*. Only minor changes on the level of the protein structure around the hemes would be required in this model. Unfortunately, no primary sequence of the *C. vinosum* subunit is available to date, so that the probability of conservation of structural elements between *R. viridis* and *C. vinosum* cannot be assessed. Such sequence information, however, has been presented for the respective subunits in *R. gelatinosus* (Nagashima et al., 1992) and *Chloroflexus aurantiacus* (Dracheva et al., 1991), showing that the essential structural elements (i.e., heme binding stretches, α-helices providing sixth ligands to the hemes) are fairly conserved whereas numerous deletions and insertions are seen within the N-terminal part and the loop extension described above. This argues against significantly different molecular conformations around the hemes of the respective subunits in different organisms and gives weight to the model implying different types of attachment.

It is of note that this model does not necessarily answer the question concerning the sequence of redox midpoint potentials in the cytochrome subunit of *C. vinosum*. Since both the $g = 3.3$ (high-potential) heme and the $g = 2.94$ (low-potential) heme are roughly parallel to the membrane, their positions are interchangeable. Only analogy to the *R. viridis* subunit would position the $g = 2.94$ (low-potential) heme closer to P than the $g = 3.3$ heme. However, to our knowledge, no experimental data have been presented so far indicating that

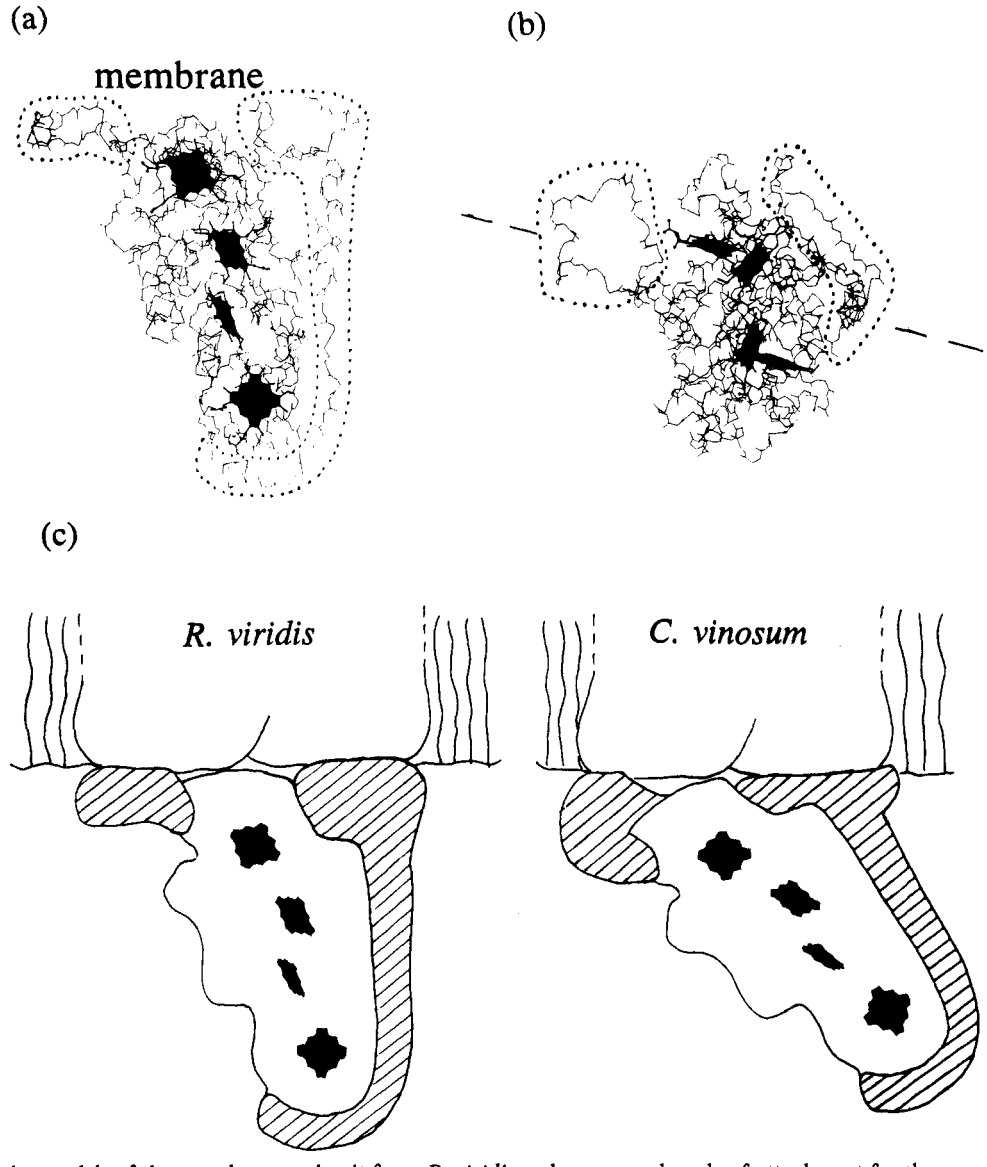

FIGURE 6: Molecular models of the cytochrome subunit from *R. viridis* and a proposed mode of attachment for the respective subunit in *C. vinosum*. (a) represents the *R. viridis* subunit as looked at from a direction parallel to the membrane plane (the membrane plane would be perpendicular to the plane of the figure). In (b), the molecule has been turned by 90° around an axis in the plane of (a) and parallel to the membrane plane. The molecule is therefore viewed from the side of the RC down toward the heme which is the most distant from the membrane. In (a) and (b), the hemes from the top to the bottom of the figure represent the hemes from the closest to the furthest position from the RC, respectively. The dashed line in (b) shows the intersection of a hypothetical plane with the plane of the figure. Alterations of the encircled sequence stretches could induce varying tilt angles of the cytochrome subunit along this hypothetical plane, as detailed in the text. For simplicity of the figure, side chains of amino acids have been omitted. (c) compares the molecular model of the *R. viridis* tetraheme subunit with a hypothetical model for the attachment of this subunit to the membrane in *C. vinosum* (and possibly also in *R. gelatinosus*). In this hypothetical model, the angle between the local C_2 axis of the tetraheme subunit and the membrane plane has been increased by 25°.

the alternating sequence of potentials seen in *R. viridis* is present also in other bacterial tetraheme cytochromes.

ACKNOWLEDGMENT

We thank Drs. G. Alegria (Philadelphia), P. L. Dutton (Philadelphia), D. B. Knaff (Lubbock), P. Mathis (Saclay), K. Matsuura (Tokyo), K. V. P. Nagashima (Tokyo), and N. Okumura (Tokyo) for stimulating discussions and for communicating results prior to publication. We furthermore acknowledge the skillful help by Drs. J. Reichert (Freiburg) and W. Leibl (Saclay) with regard to the Pdviewer software. Thanks are especially due to Dr. P. Heathcote (London) for the kind gift of *Chromatium vinosum* cells. Porphyrexide was kindly provided by Drs. M. Denis (Marseille) and H. Beinert (Milwaukee).

REFERENCES

Abola, E. E., Bernstein, F. C., Bryant, S. H., Koetzle, T. F., & Weng, J. (1987) in *Crystallographic Databases* (Allen, F. H., Bergerhoff, G., & Sievers, R., Eds.) pp 107–132, Data Commission of the International Union of Crystallography, Bonn, FRG.

Alegria, G., & Dutton, P. L. (1990) *Biophys. J. 57*, 571a.

Alegria, G., & Dutton, P. L. (1991) *Biochim. Biophys. Acta 1057*, 258–272.

Allen, J. P., Feher, G., Yeates, T. O., Rees, D. C., Deisenhofer, J., Michel, H., & Huber, R. (1986) *Proc. Natl. Acad. Sci. U.S.A. 83*, 8589–8593.

Bernstein, F. C., Koetzle, T. F., Williams, G. J. B., Meyer, E. F., Jr., Brice, M. D., Rodgers, J. R., Kennard, O., Shimanouchi, T., & Tasumi, M. (1977) *J. Mol. Biol. 112*, 535–542.

Blasie, J. K., Erecinska, M., Samuels, S., & Leigh, J. S. (1978) *Biochim. Biophys. Acta 501*, 33–52.

Blum, H., Salerno, J. C., & Leigh, J. S. (1978) *J. Magn. Reson. 30*, 385–391.
Case, G. D., & Parson, W. W. (1971) *Biochim. Biophys. Acta 253*, 187–202.
Case, G. D., & Parson, W. W. (1973) *Biochim. Biophys. Acta 325*, 441–453.
Deisenhofer, J., & Michel, H. (1989) *EMBO J. 8*, 2149–2169.
Deisenhofer, J., Epp, O., Miki, K., Huber, R., & Michel, H. (1984) *J. Mol. Biol. 180*, 358–398.
DeVault, D., & Chance, B. (1966) *Biophys. J. 6*, 825–847.
De Vries, S., & Albracht, S. P. J. (1979) *Biochim. Biophys. Acta 546*, 335–340.
Dracheva, S. M., Drachev, L. A., Konstantinov, A. A., Semenov, A. Y., Skulachev, V. P., Arutjunjan, A. M., Shuvalov, V. A., & Zaberezhnaya, S. M. (1988) *Eur. J. Biochem. 171*, 253–264.
Dracheva, S., Williams, J. C., Van Driessche, G., Van Beeumen, J. J., & Blankenship, R. E. (1991) *Biochemistry 30*, 11451–11458.
Dutton, P. L. (1971) *Biochim. Biophys. Acta 226*, 63–80.
Dutton, P. L., & Leigh, J. S., Jr. (1973) *Biochim. Biophys. Acta 314*, 178–190.
Dutton, P. L., & Prince, R. C. (1978) in *The Photosynthetic Bacteria* (Clayton, R. K., & Sistrom, W. R., Eds.) pp 525–570, Plenum Press, New York and London.
Freeman, J. C., & Blankenship, R. E. (1990) *Photosynth. Res. 23*, 29–38.
Fritzsch, G., Buchanan, S., & Michel, H. (1989) *Biochim. Biophys. Acta 977*, 157–162.
Fukushima, A., Matsuura, K., Shimada, K., & Satoh, T. (1988) *Biochim. Biophys. Acta 933*, 399–405.
Gao, J.-L., Shopes, R. J., & Wraight, C. A. (1990) *Biochim. Biophys. Acta 1015*, 96–108.
Gunner, M. R., & Honig, B. (1991) *Proc. Natl. Acad. Sci. U.S.A. 88*, 9151–9155.
Heathcote, P., & Rutherford, A. W. (1987) in *Progress in Photosynthesis Research* (Biggins, J., Ed.) Vol. I, pp 2.201–2.204, Martinus Nijhoff Publishers, Dordrecht, The Netherlands.
Jackson, J. B., & Dutton, P. L. (1973) *Biochim. Biophys. Acta 325*, 102–113.
Kihara, T., & Chance, B. (1969) *Biochim. Biophys. Acta 189*, 116–124.
Kihara, T., & Dutton, P. L. (1970) *Biochim. Biophys. Acta 205*, 196–204.
Knaff, D. B., Willie, A., Long, J. E., Kriauciunas, A., Durham, B., & Millet, F. (1991) *Biochemistry 30*, 1303–1310.
Matsuura, K., & Shimada, K. (1990) in *Current Research in Photosynthesis* (Baltscheffsky, M., Ed.) Vol. I, pp 193–196, Kluwer Academic Publishers, Dordrecht, The Netherlands.
Mims, W. B., & Peisach, J. (1976) *J. Chem. Phys. 64*, 1074–1090.
Nagashima, K. V. P., Matsuura, K., & Shimada, K. (1992) in *Meeting on Evolution of Photosynthetic Systems*, Okazaki, Japan, Poster II-6.
Nitschke, W., & Rutherford, A. W. (1989) *Biochemistry 28*, 3161–3168.
Nitschke, W., Agalidis, I., & Rutherford, A. W. (1992) *Biochim. Biophys. Acta 1100*, 49–57.
Ortega, J. M., & Mathis, P. (1992) *FEBS Lett. 301*, 45–48.
Ortega, J. M., & Mathis, P. (1993) *Biochemistry 32*, 1141–1151.
Parson, W. W. (1969) *Biochim. Biophys. Acta 189*, 397–403.
Prince, R. C., Leigh, J. S., Jr., & Dutton, P. L. (1976) *Biochim. Biophys. Acta 440*, 622–636.
Shill, D. A., & Wood, P. M. (1984) *Biochim. Biophys. Acta 764*, 1–7.
Shopes, R. J., Levine, L. M. A., Holten, D., & Wraight, C. A. (1987) *Photosynth. Res. 12*, 165–180.
Tiede, D. M. (1987) *Biochemistry 26*, 397–410.
Tiede, D. M., & Chang, C.-H. (1992) *Isr. J. Chem. 28*, 183–191.
Tiede, D. M., Leigh, J. S., & Dutton, P. L. (1978) *Biochim. Biophys. Acta 503*, 524–544.
Van Vliet, P., Zannoni, D., Nitschke, W., & Rutherford, A. W. (1991) *Eur. J. Biochem. 199*, 317–323.
Verméglio, A., Richaud, P., & Breton, J. (1989) *FEBS Lett. 243*, 259–263.
Weyer, W. R., Lottspeich, F., Gruenberg, H., Lang, F., Oesterhelt, D., & Michel, H. (1987) *EMBO J. 6*, 2197–2202.
Wood, P. M. (1980) *Biochem. J. 189*, 385–391.